A base-free synthetic route to anti-bimetallic lanthanide pentalene complexes

Article (Accepted Version)

Dalton Transactions

Accepted Manuscript

This article can be cited before page numbers have been issued, to do this please use: A. Kilpatrick and F. G. Cloke, *Dalton Trans.*, 2016, DOI: 10.1039/C6DT04475A.

ROYAL SOCIETY OF CHEMISTRY

rsc.li/dalton

View Article Online
DOI: 10.1039/C6DT04475A

Journal Name

ARTICLE

A Base-Free Synthetic Route to Anti-Bimetallic Lanthanide Pentalene Complexes†

Received 00th January 20xx,
Accepted 00th January 20xx

DOI: 10.1039/x0xx00000x

www.rsc.org/

Alexander F. R. Kilpatrick[a] and F. Geoffrey N. Cloke*[a]

We report the synthesis and structural characterisation of three homobimetallic complexes featuring divalent lanthanide metals (Ln = Yb, Eu and Sm) bridged by the silylated pentalene ligand $[1,4\text{-}\{Si^iPr_3\}_2C_8H_4]^{2-}$ (= $Pn^†$). Magnetic measurements and cyclic voltammetry have been used to investigate the extent of intermetallic communication in these systems, in the context of molecular models for organolanthanide based conducting materials.

Introduction

Multimetallic complexes of the lanthanide metals are of interest as molecular models for lanthanide-based polymers,[1,2] which have potential applications in magnetic materials,[3-6] molecular catalysis,[7,8] and luminescent devices.[9-11] The aromatic ligand pentalene $[C_8H_6]^{2-}$ (= Pn) has shown the ability to facilitate strong electronic delocalisation in anti-bimetallic transition metal compounds,[12] and promote coupling effects through the planar π-system of the bridging Pn ligand.[13-16]

The development of the silylated pentalene ligand $[1,4\text{-}\{Si^iPr_3\}_2C_8H_4]^{2-}$ (= $Pn^†$) in our laboratory, enabled the synthesis of the first pentalene bridged di-lanthanide complexes $[Cp^*Ln(THF)]_2(\mu\text{:}\eta^5,\eta^5\text{-}Pn^†)$ for Ln = Eu and Yb, *via* the one-pot reaction of $LnI_2(THF)_x$ and KCp* in THF and the subsequent addition of half an equivalent of $[K]_2Pn^†$.[17] These complexes were studied as bimetallic subsections of hypothetical lanthanide polymers $[M(Pn)]_n$, using electronic spectroscopy and cyclic voltammetry (CV). Preliminary CV studies indicated that $[Cp^*Eu(THF)]_2(\mu\text{:}\eta^5,\eta^5\text{-}Pn^†)$ decomposes readily upon oxidation but the $[[Cp^*Yb(THF)]_2(\mu\text{:}\eta^5,\eta^5\text{-}Pn^†)]^+$ mono-cation appeared to be stable under the conditions and timescale of the experiment. Furthermore through-ligand Yb–Yb coupling was suggested by the electrochemical data for $[Cp^*Yb(THF)]_2(\mu\text{:}\eta^5,\eta^5\text{-}Pn^†)$, of magnitude similar to that of its transition metal analogues.

Attempts to prepare a mixed-valence species chemically were hampered by the poor solubility of $[Cp^*Yb(THF)]_2(\mu\text{:}\eta^5,\eta^5\text{-}Pn^†)$, even in strongly coordinating solvents such as THF and DME, a problem that was sought to be remedied by the synthesis of base-free analogues. Moreover, our previous attempts to prepare the analogous Ln = Sm bimetallic by a similar synthetic route, yielded instead the monomeric sandwich complexes $(\eta^8\text{-}Pn^†)SmCp^*$ and $(\eta^8\text{-}Pn^†)Sm(\eta^5\text{-}Pn^†H)$ and the mixed-valence cluster $[Cp^*_6Sm_6(OMe)_8O][K(THF)_6]$ *via* solvent activation of THF (Scheme 1).[18] It was suggested that the strongly reducing nature of Sm(II) and the slightly larger size of this ion when compared to the smaller, less reducing Eu(II) and Yb(II), made it better stabilised, electronically and sterically, in the +3 oxidation state with $Pn^†$. Furthermore, the half-sandwich reagent used in this reaction $[Cp^*Sm(\mu\text{-}I)(THF)_2]_2$ possesses a coordinated THF molecule which can be non-innocent in reactions with highly reducing metal centres.[19-21]

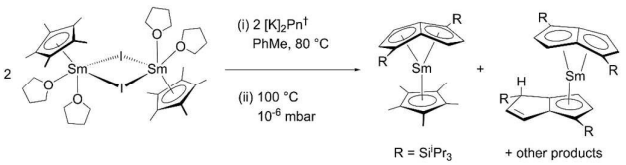

Scheme 1 Synthesis of samarium(III) pentalene sandwich compounds.[18]

Evans and co-workers reported the synthesis of mono-Cp* lanthanide(II) tetraphenylborate complexes of the type $Cp^*Ln(\mu\text{:}\eta^6,\eta^1\text{-}Ph)_2\text{-}BPh_2$, for Ln = Yb, Eu and Sm (Scheme 2).[22,23] These complexes are base-free and readily soluble in arene solvents, and therefore present alternative half-sandwich precursors to unsolvated divalent lanthanide complexes *via* salt elimination of $[M][BPh_4]$ (e.g. $M^+ = K^+$).[24] Herein, we report the synthesis and characterisation of base-free anti-bimetallic complexes $[Cp^*Ln]_2(\mu\text{-}Pn^†)$ (Ln = Yb, Eu, Sm) and studies of their electrochemical and magnetic properties.

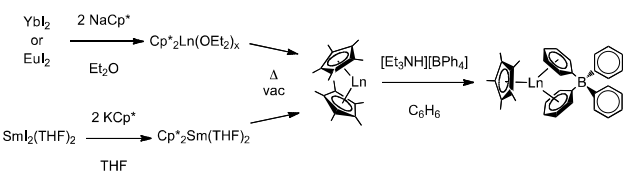

Scheme 2 Synthesis of mono-Cp* Ln(II) tetraphenylborate complexes.[22,23]

[a] *Department of Chemistry, School of Life Sciences, University of Sussex, Brighton, BN1 9QJ, UK; f.g.cloke@sussex.ac.uk*

†. Electronic Supplementary Information (ESI) available: Additional X-ray crystallographic, SQUID magnetometry and cyclic voltammetry data. CCDC 1518413–1518416. See DOI: 10.1039/x0xx00000x

View Article Online
DOI: 10.1039/C6DT04475A

Results and discussion

Synthesis and characterisation of $[Cp^*Ln]_2(\mu\text{-}Pn^{\dagger})$ complexes

The half-sandwich synthons $Cp^*Ln(BPh_4)$, for Ln = Yb and Eu,[22,23] were prepared *via* the corresponding unsolvated metallocenes,[25,26] in 46% and 59% overall yield with respect to LnI_2. The Sm(II) analogue, $Cp^*Sm(BPh_4)$, was synthesised by a similar route in 31% overall yield with respect to $SmI_2(THF)_2$.

The synthesis of the unsolvated triple-decker metallocenes, $[Cp^*Ln]_2(\mu\text{-}Pn^{\dagger})$ (Ln = Yb (**1**), Eu (**2**) and Sm (**3**)), was achieved by reaction of $Cp^*Ln(BPh_4)$ with half an equivalent of the pentalene dianion $[K]_2Pn^{\dagger}$ in toluene or benzene (Scheme 3).

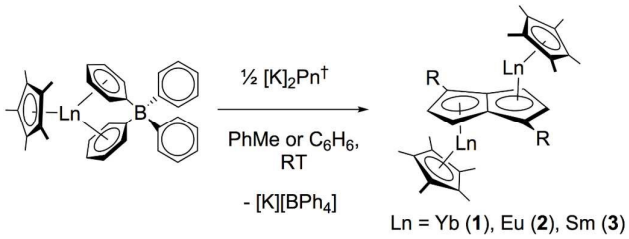

Scheme 3 General synthesis of $[Cp^*Ln]_2(\mu\text{-}Pn^{\dagger})$. R = Si^iPr_3.

This general procedure, and subsequent work-up and recrystallisation from non-coordinating solvents, afforded the base-free compounds **1**, **2** and **3** in 61, 68 and 46% yields respectively.

Compound **1** was isolated from tetramethylsilane as a brown crystalline solid, which was characterised by spectroscopic and analytical methods. Tetramethylsilane has proved to be an excellent recrystallisation solvent for complexes such as **1** which are extremely soluble in aliphatic hydrocarbons. The co-crystallised $SiMe_4$ in the molecular structure determined by single crystal X-ray diffraction (XRD) was lost from the bulk solid after rigorous drying *in vacuo*, as confirmed by microanalysis. Complex **1** was found to be diamagnetic, consistent with a ground state $4f^{14}$ configuration for each Yb(II) centre, and displays sharp peaks in its multinuclear (^1H, ^{13}C, ^{29}Si, ^{171}Yb) NMR spectra in C_6D_6 at 303 K. The ^1H NMR spectrum contains two doublet signals assigned to the aromatic $Pn^{\dagger}$ ring protons, and a singlet due to the Cp* CH_3 groups. Furthermore the triisopropylsilyl groups appear as a septet and a doublet for the C*H* and CH_3 groups respectively in the ^1H spectrum, while the $^{29}Si\{^1H\}$ spectrum shows a singlet. These observations are consistent with a solution structure on the NMR timescale that contains an inversion centre at the midpoint of the $Pn^{\dagger}$ bridgehead bond and is in agreement with the solid state structure. The $^{13}C\{^1H\}$ NMR spectrum is in agreement with this interpretation, with full assignment of resonances achieved by HSQC and HMBC experiments. The $^{171}Yb\{^1H\}$ NMR spectrum of **1** shows one signal at 59.9 ppm, consistent with two equivalent Yb(II) centres in the symmetrical anti-bimetallic, which is comparable to the other Yb(II) compounds characterised in this work as well as literature values for unsolvated ytterbocene(II) complexes (Table 1). However it should be noted that large variations in ^{171}Yb chemical shift have been reported for Cp^*_2Yb, thus making a more detailed comparison difficult.[27,28]

Table 1 Solution $^{171}Yb\{^1H\}$ NMR spectroscopic chemical shifts (δ_{Yb}) for **1** and related ytterbocene(II) complexes.

Compound	δ_{Yb} / ppm (*T* / K)	solvent	ref
1	59.9 (303)	benzene	this work
4	89.0 (303)	THF	this work
$Yb(Cp^{CH\{SiMe3\}2})_2$	118.7 (295)	toluene - benzene	29
$Yb(Cp^{\{SiMe2tBu-1,3\}2})_2$	−7.02 (304)	toluene - benzene	29
$[YbCp^*_2]_\infty$	−3.3 (298)	toluene	30
$(Cp^*Yb\{\mu\text{-}COT'''\})_2Yb$	595, 364 (298)	THF	31

Unfortunately ^{171}Yb NMR data have not been provided for the cyclooctatetrenyl (COT)-bridged bimetallic Yb(II) complexes $[Cp^*Yb]_2(\mu{:}\eta^8,\eta^8\text{-COT})$, $[Cp^*Yb(THF)](\mu{:}\eta^8,\eta^8\text{-COT})[YbCp^*]$ and $[\{(Me_3Si)_2N\}Yb(THF)]_2(\mu{:}\eta^8,\eta^8\text{-COT})$,[32-34] and multinuclear NMR spectroscopy was not possible for the THF solvate $[Cp^*Yb(THF)]_2(\mu{:}\eta^5,\eta^5\text{-}Pn^{\dagger})$ due to its low solubility. In contrast, the base-free complex **1** is highly soluble in hydrocarbon solvents, which spurred interest in studying its reactivity. Specifically, the use of non-polar solvents has been recommended for the precipitation of charged products of redox reactions,[35] which prompted our attempts to synthesise a stable mixed-valence form of this complex *via* single-electron oxidation.

Compound **2** was isolated as an orange solid from toluene-pentane solution, and was identified by single crystal XRD studies (*vide infra*) as a toluene solvate. Analytical measurements indicated that this solvent molecule remained in powdered samples that had been rigorously dried *in vacuo*, and duplicate microanalysis measurements for **2**.$(C_7H_8)_x$ best fit to x = 1.6. However, the molecular ion was observed at *m/z* = 988 in the mass spectrum (EI) with an isotopic envelope consistent with the proposed formulation. The paramagnetic nature of **2** precludes NMR analysis, giving a broad, unresolved ^1H NMR spectrum.

The relatively poor yield of the Sm(II) bimetallic **3** may be explained by a secondary product which was isolated in 22% yield, and identified by mass spectrometry (EI) and ^1H NMR spectroscopy as the known mixed-sandwich complex ($\eta^8\text{-}Pn^{\dagger}$)SmCp*.[18] An NMR scale reaction of a 2:1 mixture of $Cp^*Sm(BPh_4)$ and $[K]_2Pn^{\dagger}$ in C_6D_6 showed ^1H signals of both **3** and ($\eta^8\text{-}Pn^{\dagger}$)SmCp* after 12 h, indicating that formation of the Sm(III) by-product is inherent in the reaction conditions, rather than through adventitious oxidation. Gratifyingly, the two products can be separated by fractional crystallisation due to the lower solubility of the bimetallic complex **3** in pentane. The optimised yield (46%) was obtained by slow addition of the $Cp^*Sm(BPh_4)$ solution to a concentrated solution of $[K]_2Pn^{\dagger}$, and since **3** was found to be temperature sensitive, minimising the time the reaction mixture was kept at room temperature (< 12 h) proved beneficial. The ^1H NMR spectrum of **3** in C_6D_6 revealed a set of widely shifted signals with significant line-

View Article Online
DOI: 10.1039/C6DT04475A

broadening typical of organometallic Sm(II) complexes. Nonetheless a full assignment of the ^{1}H NMR data was made for the Cp* and Pn† ligands of complex **3** by the integration of the relevant peaks. As for **1**, the Si^{i}Pr$_3$ methyl groups were found to be chemically equivalent (i.e. non-diastereotopic) corresponding to a symmetrical bimetallic structure in solution. The ^{13}C{^{1}H} NMR spectrum for **3** shows the expected number of peaks, again paramagnetically shifted, which could not be assigned unequivocally due to the unsuitability of two dimensional ^{13}C–^{1}H correlation experiments for this paramagnetic complex. The molecular ion was observed at *m/z* = 985 in the mass spectrum (EI) with an isotopic envelope in good agreement with the proposed formulation.

X-ray crystallographic studies

Anti-bimetallic complexes **1**, **2** and **3** were characterised in the solid state by single crystal XRD, and views of their molecular structures are depicted in Figure 1. Complex **1** crystallises in the monoclinic space group $P2_1/c$ with one half-molecule in the asymmetric unit, whereas **3** crystallises in the triclinic space group *P*–1 and contains two independent half-molecules, each with different structural parameters, which are compared in Table 2.

Compounds **1** and **3** are not isomorphous, but are similar in many respects. In the solid state both anti-bimetallics exhibit a slipped triple-decker arrangement and an η^5,η^5 metallocene-like bonding mode. They are symmetrical and possess an inversion centre at the midpoint of the bridgehead carbons, which results in a 180° Ct(Cp*)–M–M–Ct(Cp*) torsional angle. The pentalene and Cp* ligands are planar but not mutually coplanar, instead adopting a bent arrangement of rings around the metal, as is well-known for the divalent lanthanide metallocenes.[25,36,37] The extent of bending in these compounds, as well as their alkaline earth analogues, has been related to metal size.[38] Complexes of the smallest metals, which have the rings closest together, have the most linear structures. The Ct(Cp*)–M–Ct(Pn) angles for **1** and **3** follow this trend, reflecting the smaller ionic radius of the Yb^{2+} centre compared with Sm^{2+} (r_{Ln2+} = 1.02 and 1.22 Å respectively for 7-coordinate ions).[39] This angle in **1** (139.31(8)°) is larger than that in the THF solvated analogue [Cp*Yb(THF)]$_2$(μ:η^5,η^5-Pn†) (138.2(2)°), just as the Ct(Cp*)–M–Ct(Cp*) angle in Cp*$_2$Yb (145.0°) is larger than in solvated Cp*$_2$Yb(THF) (143.5(3)°).[40] For comparison, the Ct(Cp*)–M–Ct(Cp*) angles are 140.1° in unsolvated Cp*$_2$Sm,[36] and 136.7° in solvated Cp*$_2$Sm(THF)$_2$.[41] Slight differences between the structures are found in the ligand-metal bonding distances and reflect the variation in metal ionic radii. The smaller Yb(II) centre is found to allow closer coordination of the carbocyclic ligands in **1** compared to **3**, M–Ct(Pn) = 2.389(3) and av. 2.492(4) Å, M–Ct(Cp*) = 2.389(3) and av. 2.496(5) Å, respectively. The average M–C$_{ring}$(Cp*) distances are comparable to those in the corresponding triple-decker [Cp*Ln]$_2$(μ:η^8,η^8-COT), [Cp*Ln]$_2$ μ:η^8,η^8-COT†) (COT† = [C$_8$H$_6${Si^{i}Pr$_3$-1,4}$_2$]$^{2-}$), and Cp*$_2$Ln complexes.[17,25,32,42-44]

Each asymmetric unit of **1** contains one co-crystallised SiMe$_4$ molecule which is orientated towards Yb1 from the open side of the metallocene wedge, and the shortest M···C(methyl) distance (2.930(6) Å) is less than the sum of the van der Waals radii (3.7 Å). Complex **3** is solvent free and the open face of the metallocene wedge is approached by one of the Si^{i}Pr$_3$-methyl groups from an adjacent molecule, with close intermolecular M···C(methyl) contacts of 3.435 and 3.394(10) Å for Sm1 and Sm2 respectively. Additionally, all three structures **1**, **2** and **3** show close intramolecular contact between the Ln(II) centres and one of the methyls of the pentalene Si^{i}Pr$_3$ groups (Table 2), as often occurs in lanthanide complexes with N(SiMe$_3$)$_2$ ligands.[45-49] Complex **2** has a solid state molecular structure in which the two europium centres occupy radically different coordination environments. Eu1 is in the expected bent η^5,η^5-metallocene configuration, with M–Ct(Pn) and Ct(Cp*) distances and angles similar to those found in the THF solvate [Cp*Eu(THF)]$_2$(μ:η^5,η^5-Pn†) (2.502(6) Å, 2.477(5) Å, and

Table 2 Selected distances (Å), angles (°), and parameters (defined in ESI†) for **1**, **2** and **3**. Ct1 and Ct2 correspond to the η^5,η^5-centroids of the Pn ring. Ct3 and Ct4 correspond to the η^5-centroids of the Cp* rings.

Parameter	1	2	3
M···M	5.230(2)	5.1627(5)	5.2737(12), 5.3973(6)
M1–Ct1	2.389(3)	2.569(2)	2.476(4), 2.508(4)
M1–Ct3	2.397(3)	2.515(2)	2.493(5), 2.498(5)
M2–Ct1	-	2.638(2)	-
M2–Ct2	-	2.5081(18)	-
M2–Ct4	-	2.540(2)	-
$\Delta_{M1\text{-}Ct1}$	0.052	0.069	−0.047, 0.006
$\Delta_{M2\text{-}Ct2}$	-	−0.268	-
Ct1–M1–Ct3	139.31(8)	131.82(7)	133.711(6), 135.06(9)
Ct1–M2–Ct4	-	157.54(7)	-
Ct2–M2–Ct4	-	153.15(7)	-
av. Pn C–C$_{ring}$	1.437(7)	1.435(5)	1.435(14), 1.434(14)
M–C$_{agostic}$ [a]	3.1399(5)	3.114(6)	3.278(10), 3.359(11)
Fold angle	0.0	16.1(2)	0.0, 0.0

[a] Shortest M–^{i}Pr *C*H$_3$ distance within each independent molecule.

View Article Online
DOI: 10.1039/C6DT04475A

Journal Name

ARTICLE

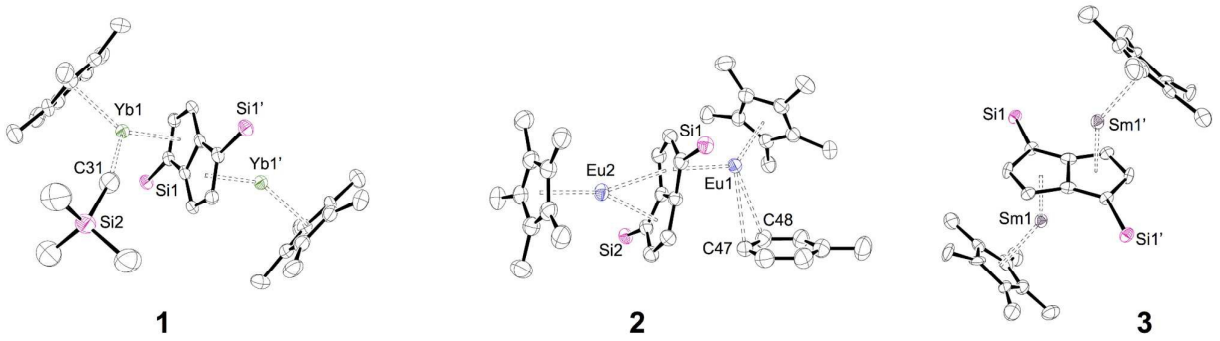

Figure 1 Displacement ellipsoid plots (50% probability) of $[Cp^*Ln]_2(\mu\text{-}Pn^{\dagger})$, Ln = Yb (**1**), Eu (**2**), Sm (**3**). H atoms and ^{i}Pr groups omitted for clarity. Atoms marked with a prime are generated by symmetry, with one molecule of $SiMe_4$ omitted for **1**, and one of the asymmetric units of **3** omitted for clarity.

131.5(2)° respectively).[17] There is also an interaction between Eu1 and the molecule of co-crystallised toluene located in the structure, with two short contacts, to C47 and C48 of 3.060(5) and 3.214(5) Å respectively, which lie within the range of Eu–C distances in previously reported Eu complexes with neutral π-arenes (2.965–3.266 Å).[50,51] The rest of the distances between Eu1 and this phenyl ring are greater than 3.6 Å and are not considered significant.

In contrast the other europium atom Eu2 is not solvated but interacts with all 8 carbons of the pentalene ring, which folds by 16.1° to accommodate the electropositive centre, as is typical for the structures of *mono* f-element pentalene compounds.[18,52] This unusual coordination environment for Eu2 is quantified by the ring slippage parameter (−0.268 Å) with its proximal pentalene C_5-centroid (see ESI† Figure S1 for definition of Δ_{M-Ct}) which is exceptionally large and negative in comparison to this parameter for Eu1 (0.069 Å), and those for **1** and **3**.

Pentalene is normally considered as a dianionic ligand in the η^8- bonding mode to a single metal centre, and monoanionic in η^5- mode,[53] which would indicate, *prima facie*, a +3 oxidation state for Eu2. However, SQUID magnetometry measurements (*vide infra*) are fully consistent with a +2 oxidation state of each Eu centre in **2**. Furthermore, addition of THF to **2** was shown by IR spectroscopy (*vide infra*) to yield the solvated complex $[Cp^*Eu(THF)]_2(\mu\text{-}Pn^{\dagger})$ in which the bridging pentalene ligand adopts the expected η^5,η^5- binding mode in the solid state, leaving no ambiguity in the divalent state for each Eu. The distance between Eu2 and the distal pentalene C_5-centroid in the molecular structure of **2** (2.638(2) Å) is longer than in any Ln–Ct(Pn) formal bonding distance reported to date,[12] and is thus best considered as a subtle interaction attributed to the electron deficiency of Eu2 with respect to Eu1. A list of short intermolecular contacts (less than the sum of the van der Waals radii), and a displacement ellipsoid plot of the unit cell of **2** are included in the ESI.

Magnetic studies

The magnetic susceptibility of **2** and **3** was studied in solution using the Evans method[54,55] and in the solid state using SQUID magnetometry. The magnetic properties of lanthanide ions due to unpaired 4f electrons are generally well described by the coupling of spin (*S*) and orbital (*L*) angular momenta in the Russell-Saunders coupling scheme to give a total angular momentum (*J* = *L* + *S*). Spin-orbit coupling constants (*ca.* 1000 cm^{-1}) are typically much larger than ligand-field splittings (*ca.* 100 cm^{-1}) so that only the ground *J* state is thermally populated. Using these assumptions the effective magnetic moment (μ_{eff}) is given by the Landé formula, $\mu_{eff} = g_J[J(J+1)]^{½}$, where, g_J is the Landé *g*-factor.[56]

Divalent europium ions have a $4f^7$ configuration with term symbol ^8S. The effective magnetic moment (μ_{eff}) of **2** in C_6D_6 solution was 7.64 μ_B per M at 303 K, which is in reasonable agreement with the value for the Eu^{2+} free ion calculated using the Landé formula (7.94 μ_B). The temperature dependence of the solid state magnetism of powdered crystalline **2**.$(C_7H_8)_{1.6}$ was measured between 2 – 300 K. The majority of paramagnetic substances have a molar susceptibility (χ_m) that obeys the Curie-Weiss law, $\chi_m = C/(T - \Theta)$, where *C* is the Curie constant and Θ is the Weiss constant. The plot of χ_m^{-1} vs *T* for **2** (Figure 2) follows Curie-Weiss behavior from 16 – 300 K, with *C* = 7.415 K^{-1} mol^{-1} and Θ = −1.5 K. This corresponds to a μ_{eff} of 7.68 μ_B per M at 300 K which is comparable with that of monomeric metallocenes Cp_2Eu (7.63 μ_B) and Cp^*_2Eu (7.70 μ_B),[26] suggesting that at these temperatures **2** behaves as two

View Article Online
DOI: 10.1039/C6DT04475A

non-interacting Eu^{2+} centres. The observed intramolecular Eu···Eu distance (5.1627(5) Å) is relatively long compared with the analogous $COT^{\dagger}$ complex, $[Cp^*Eu]_2(\mu\text{-}COT^{\dagger})$ (4.293(5) Å),[17] and may explain the lack of magnetic interactions. However, Murugesu and co-workers have recently shown that the anti-bimetallic complexes, $[COT'Ln]_2(\mu{:}\eta^8,\eta^8\text{-}COT')$ (Ln = Dy, Er; COT' = $[C_8H_6\{SiMe_3\text{-}1,4\}_2]^{2-}$),[4,57] have a non-negligible interaction between Ln^{3+} centres which is facilitated by the bridging COT' ligand. Furthermore, long range ferromagnetic f-f interactions have been reported by Fukuda *et al.* in heterobimetallic quadruple-decker phthalocyanine complexes containing Y^{3+}/Dy^{3+} or Y^{3+}/Er^{3+} ions at distances up to 6.8 Å.[58] Field dependent magnetisation measurements from 0.1 to 5 Tesla (see ESI† Figure S4) reveal that at 16 K, the magnetisation (*M*) of **2** increases almost linearly with applied field, as expected for a paramagnetic system in which interactions between neighbouring ions are weak. At lower temperatures, *M* no longer increases linearly with *H*, and takes the form of a curve described by the Brillouin function.[59] The *M* vs *H* curve at 2 K approaches a limiting value at 5 Tesla, which is the saturation magnetisation of the sample when all of the spins have aligned.

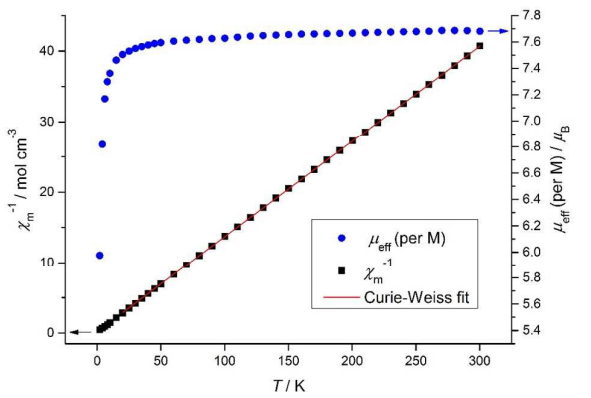

Figure 2 Temperature dependence of the solid state μ_{eff} and χ_m^{-1} for **2** at 1 Tesla.

The Sm^{2+} ion is a $4f^6$ ion with term symbol $^7F_0$, which is a special case, in that the Landé formula predicts (incorrectly) a μ_{eff} of zero, hence f^6 ions Sm^{2+} and Eu^{3+} were termed *anomalous* by Van Vleck.[59] For these ions the separation of the $J = 0$ and $J = 1$ states is *ca.* 300 cm^{-1}, and the $J = 1$ and $J = 2$ states is *ca.* 200 cm^{-1}, both of which are of the order of k_BT.[26] This means at normal temperatures there must be a significant population of the excited multiplet states, and this immediately invalidates the Landé formula.[56]

The solution magnetic moment of **3** in toluene-d_8 was 3.04 μ_B per M at 303 K. SQUID measurements revealed a complex temperature dependence of the solid state susceptibility between 2 – 300 K. The χ_m^{-1} vs *T* plot (Figure 3) has a shallow slope below 40 K, suggesting that at these temperatures, when most of the electrons are in the ground state, complex **3** behaves as a temperature independent paramagnet. However, as *T* increases the $J = 1$ and $J = 2$ states become increasingly populated, so that at 300 K μ_{eff} has increased to a value of 3.09 μ_B per M. The plot of χ_m^{-1} vs *T* for **3** is comparable to those for the monomeric samarium metallocenes $Cp^*_2Sm(THF)(OEt_2)$ and Cp^*_2Sm,[26] as well as those found for simple Eu^{3+} salts, which are also f^6 ions.[60,61] There are no features of the χ_m^{-1} vs *T* plot that indicate intramolecular interactions between the two paramagnetic centres. This is somewhat expected based on the relatively long intramolecular Sm···Sm distance (av. 5.336 Å) found in the molecular structure and the poor radial extension of 4f orbitals, which typically results in weak exchange coupling between lanthanide ions.[2] Fitting a straight line to χ_m^{-1} vs *T* in the Curie-Weiss regime (between 100 – 300 K) gives $C = 1.881$ K^{-1} mol^{-1}, $\Theta = -161.1$ K and a μ_{eff} of 3.09 μ_B per M at 282 K, which is comparable with the solid state susceptibility of Cp^*_2Sm (3.36 μ_B) reported at this temperature.[26] Field-dependent measurements (see ESI† Figure S5) further illustrate that the magnetisation of **3** is temperature independent at 32 K and below, and the near-linear dependence of the magnetisation with applied field confirms that intermolecular interactions are weak.

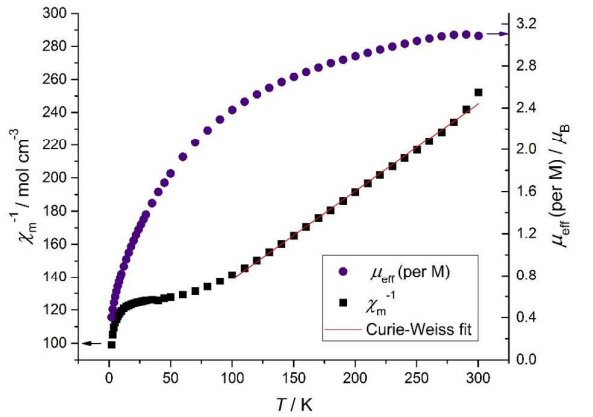

Figure 3 Temperature dependence of the solid state μ_{eff} and χ_m^{-1} for **3** at 0.1 Tesla.

Electrochemical studies

Cyclic voltammetry (CV) is a powerful technique for investigating the electronic properties of organometallic complexes.[62] In f-element chemistry CV is commonly used to rationalise trends in reactivity arising from a different set of ligands on a common metal or vice versa. The thermodynamic trend in 3+/2+ reduction potentials for Yb and Sm complexes is expected to follow that of the Ln^{3+} ions in acidic aqueous media,[63] with the latter metal *ca.* 0.5 V more reducing than the former. However, direct observation of the reverse process, i.e. $Ln^{2+/3+}$ oxidation, is complicated by the high reactivity of Ln(II) complexes and the fact that the expected redox event lies outside the potential window of many solvent/electrolyte systems commonly used in organotransition metal chemistry. Nonetheless mid-peak potential ($E_{½}$) values have been determined by CV in select examples of Ln(II) metallocenes

View Article Online
DOI: 10.1039/C6DT04475A

which show appreciable stability in the chosen electrolytic medium (Table 3).

Table 3 Mid-peak potentials ($E_{½}$) vs $FeCp_2^{+/0}$ of the Ln(III)/Ln(II) couple in divalent lanthanide metallocenes with a [^{n}Bu$_4$N][A] supporting electrolyte.

Complex	$E_{½}$ ($Ln^{3+/2+}$) / V	solvent	electrolyte $[A]^-$	ref
Cp^*_2Yb	−1.48	THF	$[B(C_6F_5)_4]$	64
$(Cp^{Me4Et})_2Sm$	−2.12	THF	$[B(C_6F_5)_4]$	65
Cp^*_2Yb	−1.78	MeCN	$[PF_6]$	66
Cp^*_2Eu	−1.22	MeCN	$[PF_6]$	66
Cp^*_2Sm	−2.41	MeCN	$[PF_6]$	66

Complexes **1** and **2** are readily soluble in hydrocarbon solvents (*ca.* 0.1 mmol cm^{-3} in benzene) with respect to their THF solvated analogues, however finding a suitable solvent/electrolyte system compatible for comparative electrochemical studies for these complexes and **3** proved non-trivial. The Sm(II) complex **3** reacts with THF over the course of 12 h, however reasonable CV data were obtained in this solvent when measured within a 1 h period after dissolution. Using [^{n}Bu$_4$N][PF_6] supporting electrolyte, two processes were observed within the electrochemical window (Figure 4).

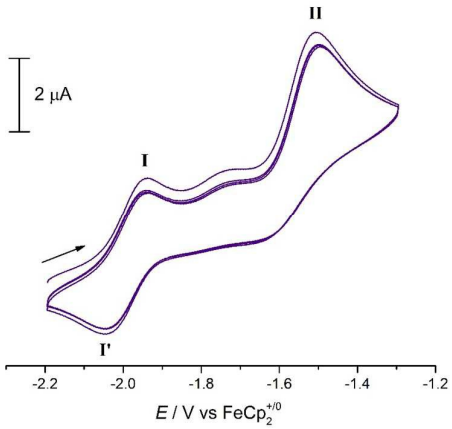

Figure 4 Overlaid CV scans (3 cycles) for **3** in THF / 0.1 M [^{n}Bu$_4$N][PF_6], scan rate 50 mV s^{-1}.

Process I, with a mid-peak potential ($E_{½}$ = {E_{pa} + E_{pc}}/2) of −2.0 V vs $FeCp_2^{+/0}$ (a convention which is assumed for all potentials quoted henceforth), is tentatively assigned to a [Sm^{II}-Sm^{II}]/[Sm^{III}-Sm^{II}] oxidation on the basis of comparable values of the Sm(III/II) couple in this solvent.[65] Repetitive potential cycling over process I in isolation using varied scan rates (50 to 500 mV s^{-1}), showed electrochemical behaviour best described as quasi-reversible.[67] The peak-to-peak separation (ΔE_{pp}) was comparable to that for ferrocene under the same conditions (*ca.* 120 mV), suggesting that only one electron is being transferred. Process II shows an anodic wave with a peak potential (E_{pa}) of −1.5 V in the forward scan, however no associated cathodic wave was observed in the reverse scan. Irreversible behaviour suggests that the product of this second oxidation is not stable under the conditions and timescale of the experiment. It is noted that process I shows a lower current response than process II. Due to the highly negative region of the potential window which at these processes occur, it may be that appreciable oxidation of the Sm(II) species had occurred prior to application of the initial potential of the forward scan (−2.2 V). After a period of *ca.* 1 h, the current response of process I diminished almost entirely and additional anodic waves appeared upon scanning to more positive potentials. Presumably after this period the Sm(II) species has nearly completely decomposed, consistent with ^{1}H NMR spectroscopy observations.

The electrochemical behaviour of **3** in THF/[^{n}Bu$_4$N][PF_6], is qualitatively comparable to that previously reported for [Cp*Yb(THF)]$_2$(μ:η^5,η^5-Pn†) in THF/[^{n}Bu$_4$N][B(3,5-{CF_3}$_2$$C_6H_3$)$_4$],[17] which shows a quasi-reversible oxidation to the mono-cation followed by irreversible behaviour in the second oxidation. For a better comparison, CV studies of **3** were attempted using the alternative weakly coordinating electrolyte [^{n}Bu$_4$N][$B(C_6F_5)_4$] in THF,[68] however the voltammograms obtained were distorted due to high solution resistance. Inspection of the gold disc working electrode showed solid deposits on the surface, indicative of electrode fouling.

The CV data for [Cp*Ln]$_2$(μ-Pn†) complexes **1**, **2** and **3** are given in Table 4. The oxidative potentials follow the thermodynamic trend for reducing power Sm > Yb > Eu,[63] although a more in-depth comparison cannot be made due to the different electrolytic media used. Furthermore, the peak separations between the oxidation waves (ΔE) does not represent the difference between mid-peak potentials (hence not designated $\Delta E_{½}$), and hence the value does not represent a true thermodynamic measurement of the comproportionation equilibrium constant (K_c) for the mixed-valence mono-cation.

Table 4 Electrode potentials vs $FeCp_2^{+/0}$ for **1–3** in different supporting electrolytes.

Complex	$E^{(1)}$ / V	$E^{(2)}$ / V	$\Delta E^{(2)-(1)}$ / V	electrolyte	ref
1	−1.9	−1.5[a]	0.4	[b]	17
1	−1.7[a]	−1.3	0.5	[c]	this work
1	−1.7	−1.5	0.2	[d]	this work
2	−1.4[a]	−1.1[a]	0.3	[b]	17
3	−2.0	−1.5 [a]	0.5	[e]	this work

[a] Anodic peak potentials (E_{pa}) are quoted for irreversible processes. [b] THF / 0.1 M [^{n}Bu$_4$N][B(3,5-{CF_3}$_2$$C_6H_3$)$_4$] [c] THF / 0.1 M [^{n}Bu$_4$N][$B(C_6F_5)_4$] [d] MeCN / 0.1 M [^{n}Bu$_4$N][PF_6] [e] THF / 0.1 M [^{n}Bu$_4$N][PF_6].

Redox reactions

The CV measurements reveal the potential for oxidation of [Ln^{II}-Ln^{II}] complexes **1**, **2** and **3**. With these values in hand, the synthesis of a mixed-valence [Ln^{III}-Ln^{II}] complex was attempted on a preparative scale. Complex **1** was selected for preliminary reactivity studies for the series. It was envisaged that the milder reducing potential for Yb(II)

View Article Online
DOI: 10.1039/C6DT04475A

compared with Sm(II) may result in a stable mixed-valence complex.

Reaction of **1** with one equivalent of $[FeCp^*_2][B(C_6F_5)_4]$ in Et_2O at −40 °C resulted in an orange solution. Following evaporation of the solvent and removal of $FeCp^*_2$ by washing with pentane, the residues were recrystallised from Et_2O/TMS_2O at −35 °C yielding $[Cp^*Yb(OEt_2)_3][B(C_6F_5)_4]$ (**4**) as a yellow solid (Scheme 4). Ion-pair **4** was characterised by NMR spectroscopy, elemental analysis and X-ray crystallography.

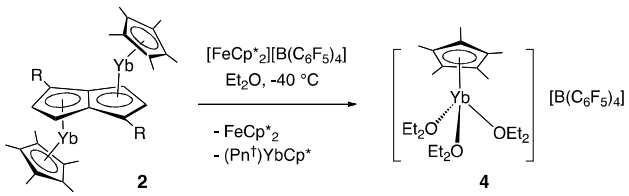

Scheme 4 Oxidation of **1** with $[FeCp^*_2][B(C_6F_5)_4]$. R = Si^iPr_3.

The ^1H NMR spectrum shows a resonance for the Cp* methyl groups at 1.97 ppm, and coordinated Et_2O appears at 3.38 and 1.11 ppm. Relative integration of these peaks indicated the presence of 3 moles of Et_2O per Cp* ligand. The tetrakis(perfluorophenyl)borate counter anion is easily identified by a sharp singlet in the $^{11}B\{^1H\}$ spectrum at −14.7 ppm and three signals at −130, −163.3 and −166.8 ppm in the ^{19}F spectrum for the *o*, *p* and *m*-F respectively.

The solid state structure (Figure 5) shows a mononuclear half-sandwich Yb(II) cation, $[Cp^*Yb(OEt_2)_3]^+$, and an outer-sphere $[B(C_6F_5)_4]^-$ anion, each displaying a distorted tetrahedral geometry about the central atoms (Yb1 and B1 respectively). The Yb and B atoms of the ion-pair **4** are separated by 8.128(6) Å, in contrast to ytterbium(II) tetraphenylborate complexes $[(N\{SiMe_3\}_2)Yb(THF)BPh_4]$,[69] $[(^tBu_2pz)Yb(THF)BPh_4]$,[70] and $Cp^*Yb(BPh_4)$[22] in which two of

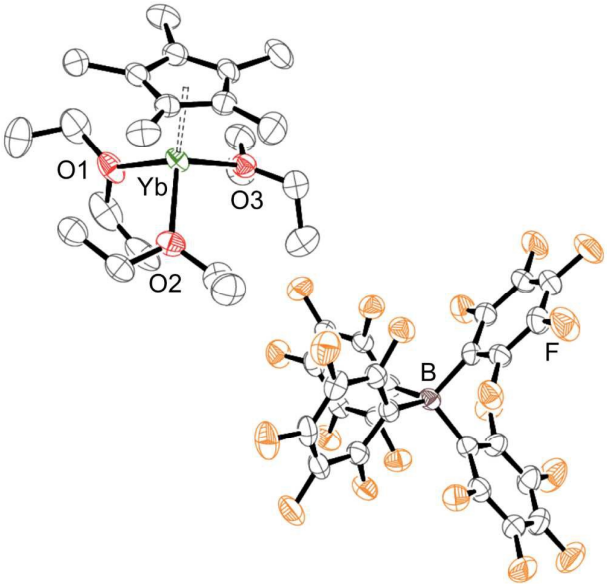

Figure 5 Displacement ellipsoid plot (50% probability) of **4** with H atoms omitted for clarity. Selected interatomic distances (Å) and angles (°): Yb1–Ct1 = 2.369(2), Yb1···Ct2 = 6.769(3), Yb1–O1 = 2.404(3), Yb1–O2 = 2.394(3), Yb1–O3 = 2.383(3), Yb1···B1 = 21.175(7), O1–Yb1–O2 = 104.43(11), O1–Yb1–O3 = 90.74(13), O2–Yb1–O3 = 111.06(12), O1–Yb1–Ct1 = 122.61(12), O2–Yb1–Ct1 = 113.62(9), O3–Yb1–Ct1 = 112.07(9). Ct1 denotes the η^5-centroid of the Cp* ligand. Ct2 denotes the ring centroid of the proximal C_6F_5 group.

the phenyl rings of the anion can bind in an η^6-mode to the metal centre, resulting in closer Yb···B distances of 3.690(3), 3.636(2) and 3.708(5) Å respectively.

Presumably the second Yb-containing product in this reaction is the mixed-sandwich compound (η^8-$Pn^†$)YbCp*, which is expected to be readily soluble in pentane, and hence extracted with the decamethylferrocene fraction. Evans and co-workers have reported the synthesis of the related mixed-sandwich compound, (η^8-COT)YbCp*, by addition of cyclooctatetraene to $[Cp^*Yb]_2(\mu\text{-}\eta^8\text{:}\eta^8\text{-COT})$.[32] Repeating the reaction of **1** with one equivalent of $[FeCp^*_2][B(C_6F_5)_4]$ in Et_2O at −40 °C, followed by removal of the solvent and decamethylferrocene *via* vacuum sublimation resulted in a equimolar mixture of **4** and (η^8-$Pn^†$)YbCp*, as identified by mass spectrometry and multinuclear (^1H, ^{13}C, ^{11}B, ^{19}F, ^{29}Si, ^{171}Yb) NMR spectroscopy. Despite the relatively mild oxidising power of the decamethylferrocenium ion (measured as $E_{½}$= −0.52 V in THF/0.1 M $[^nBu_4N][B(C_6F_5)_4]$), its reaction with **1** leads to dissociation rather than stabilisation of the mixed-valence bimetallic. Previous attempts using more potent oxidising agents such as $[Cp_2Fe][B(3,5\text{-}\{CF_3\}_2C_6H_3)_4]$ and $[Ag][BPh_4]$ failed to give tractable products.[17] It is proposed that the η^5- and η^8- bonding modes that are available to the pentalene dianion are detrimental to the formation of bridged bimetallic species such as $[Cp^*Ln(\mu\text{-}Pn^†)LnCp^*]^+$, since the +3 oxidation state is better stabilised in mononuclear sandwich compounds of the type (η^8-$Pn^†$)LnCp*, leading to dissociation (Scheme 5).

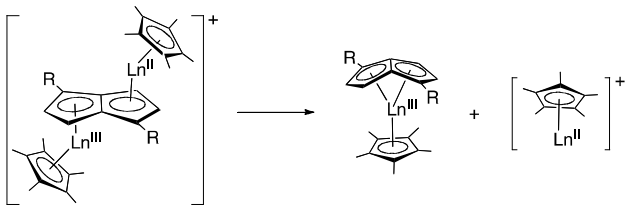

Scheme 5 Possible decomposition pathway of mixed-valence bimetallic. R = Si^iPr_3.

In an attempt to prepare an authentic sample of (η^8-$Pn^†$)YbCp* *via* a direct, one-pot route, YbI_3 was reacted with KCp* and $[K]_2Pn^†$ in THF. Subsequent work-up and recrystallisation from pentane furnished the homoleptic complex $[(\eta^8\text{-}Pn^†)_2Yb][K]$ (**5**) in 15% yield, as identified by elemental analysis and mass spectrometry. ^1H NMR spectroscopy in THF-d_8 showed broad signals consistent with a paramagnetic Yb(III) (f^{13}) complex which could be assigned to the $Pn^†$ ligand by relative integration ratios. X-ray crystallography established the connectivity of the

View Article Online
DOI: 10.1039/C6DT04475A

atoms in **5** as the 'ate' complex shown Figure S3 of the ESI, however the low quality of the data precluded accurate refinement of metric parameters. There is precedent for such Ln(III) anionic bis(pentalene) sandwich complexes with Ln = Ce,[71,72] emphasising the steric and electronic stabilisation achieved for the f-elements with the pentalene ligand in η^8-mode.

Conclusions

The synthesis of anti-bimetallic complexes of the divalent lanthanides was investigated, with the half-sandwich Cp*Ln(BPh_4) precursor allowing for the preparation of base-free complexes [Cp*Ln]$_2$(μ-Pn†) for Ln = Yb (**1**), Eu (**2**) and Sm (**3**). Isolation of latter compound is notable, given that it could not be prepared by a similar method using the [Cp*Sm(μ-I)(THF)$_2$]$_2$ half-sandwich precursor, due to THF activation. The Ln(II) anti-bimetallic complexes were characterised by single crystal XRD analysis, which revealed similarities between the symmetrical structures **1** and **3**, and those of the known THF solvates [Cp*Ln{THF}$_2$]$_2$(μ-Pn†) (Ln = Yb and Eu). Unexpectedly, **3** showed a solid state molecular structure in which one Eu centre interacts with a co-crystallised toluene molecule and the other Eu centre interacts with all 8 carbons of the Pn† ring. Paramagnetic complexes **2** and **3** were studied by variable temperature and field SQUID magnetometry, which revealed very similar magnetic behaviour to their respective mononuclear Cp*$_2$Ln(II) complexes. The lack of magnetic interaction between the metal centres may be explained by the large Ln···Ln distance (> 5 Å) and the 'core-like' radial distribution of f-orbitals.

Electrochemical studies of [Cp*Ln]$_2$(μ-Pn†) were complicated by their reactivity with polar solvents. The Sm(II) complex **3** showed sufficient stability in THF/[^{n}Bu$_4$N][PF_6] over 1 h, and its CV was qualitatively comparable to that for the Yb(II) complex studied in this solvent. In each case the first oxidation processes had some reversibility, with $E_{½}$ values that are consistent with the thermodynamic trend for the $Ln^{3+/2+}$ couple. However the second process was irreversible, suggesting that the product of this second oxidation is not stable under the conditions and timescale of the experiment.

Attempted synthesis of a mixed-valence [Ln^{III}-Ln^{II}] complex by chemical oxidation of **1** with [FeCp*$_2$][B(C_6F_5)$_4$] lead to dissociation and a mononuclear half-sandwich cation **4**, was isolated and structurally characterised.

Experimental details

General procedures

All manipulations were carried out using standard Schlenk techniques under Ar, or in an MBraun glovebox under N_2 or Ar. All glassware was dried at 160 °C overnight prior to use. Solvents were purified by pre-drying over sodium wire and then distilled over Na (toluene, TMS_2O), K (THF, hexane, C_6H_6, ^{t}BuOMe, DME) Na-K alloy (Et_2O, pentane, $SiMe_4$), or CaH_2 (CH_2Cl_2, 1,2-difluorobenzene, MeCN) under a N_2 atmosphere. Dried solvents were collected, degassed and stored over argon in K mirrored ampoules, except THF, Et_2O, C_6H_6, CH_2Cl_2, 1,2-difluorobenzene and MeCN which were stored in ampoules containing activated 4 Å molecular sieves. $SiMe_4$ was stored over activated 4 Å molecular sieves at −35 °C in the glovebox. Deuterated solvents were degassed by three freeze–pump–thaw cycles, dried by refluxing over K for 3 days, vacuum distilled into ampoules and stored under N_2. The compounds [K]$_2$Pn†,[73] KCp*,[74] NaCp*,[74] [Et_3NH][BPh_4],[75] Cp*$_2$Yb(OEt_2)$_2$,[76] Cp*$_2$Sm(THF)$_2$,[44] Cp*$_2$Sm,[36] Cp*$_2$Yb, Cp*$_2$Eu,[36] Cp*Sm(BPh_4), Cp*Yb(BPh_4),[22] and Cp*Eu(BPh_4)[23] were prepared according to published procedures. Reagents YbI_2, YbI_3, EuI_2 and [FeCp*$_2$][B(C_6F_5)$_4$] were kindly donated by co-workers. NMR spectra were measured on Varian VNMRS 400 (^{1}H 399.5 MHz; ^{13}C{^{1}H} 100.25 MHz; ^{29}Si{^{1}H} 79.4 MHz) or VNMRS 500 (^{1}H 499.9 MHz; ^{13}C{^{1}H} 125.7 MHz) spectrometers. The spectra were referenced internally to the residual protic solvent (^{1}H) or the signals of the solvent (^{13}C). ^{11}B, ^{19}F, ^{29}Si and ^{171}Yb NMR spectra were referenced externally relative to BF_3.OEt_2, $CFCl_3$ (10%), $SiMe_4$, and YbCp*$_2$ (in 10% THF/C_6D_6) respectively. IR spectra were recorded between NaCl plates using a Perkin-Elmer Spectrum One FTIR instrument. Mass spectra were recorded using a VG Autospec Fisons instrument (EI at 70 eV). Elemental analyses were carried out at the Elemental Analysis Service, London Metropolitan University. Additional elemental analyses for compounds **2** and **3** were carried out at the analytical laboratories of the Friedrich-Alexander-University (FAU) Erlangen-Nürnberg on Euro EA 3000, prior to SQUID magnetometry measurements. Magnetic measurements of polycrystalline samples of **1**, **2** and **3** were carried out at FAU Erlangen and the University of Oxford, using a Quantum Design MPMS-5 SQUID magnetometer at different fields (0.1 – 5 Tesla) and different temperatures (2 – 300 K). Accurately weighed samples (*ca.* 30 mg) were placed into gelatine capsules and then loaded into nonmagnetic plastic straws before being lowered into the cryostat. Data reproducibility was carefully checked on two independently synthesised and measured samples. Solution phase magnetic susceptibilites were determined using the Evans method,[54,55] and measured on the Varian VNMRS 400 MHz spectrometer. Samples were allowed 15 min to thermally equilibrate at the given probe temperature which was calibrated with a methanol thermometer. The solvent density at the given temperature was factored in to the magnetic susceptibility calculation.[77,78] Cyclic voltammetry studies were carried out using a BASi Epsilon-EC potentiostat under computer control. *iR* drop was compensated by the feedback method. CV experiments were performed in an Ar glovebox using a three-electrode configuration with a Au disc (2.0 mm^2) or glassy carbon disc (7.0 mm^2) as the working electrode, a Pt wire as the counter electrode and a Ag wire as the pseudoreference electrode. Sample solutions were prepared by dissolving the analyte (*ca.* 5 mM) in THF (1.0

View Article Online
DOI: 10.1039/C6DT04475A

cm^3) followed by addition of a supporting electrolyte [^{n}Bu$_4$N][B(C$_6$F$_5$)] or [^{n}Bu$_4$N][PF$_6$]. The reported mid-peak potentials are referenced internally to that of the $FeCp_2^{+/0}$ redox couple, which was measured by adding ferrocene (*ca.* 1 mg) to the sample solution.

Syntheses

Synthesis of [Cp*Yb]$_2$(μ:η^5,η^5-Pn†) (1)

[K]$_2$Pn† (580 mg, 1.18 mmol) in benzene (20 mL) was added portionwise to a green solution of Cp*Yb(BPh$_4$) (1.479 g, 2.357 mmol) in benzene (50 mL) at room temperature and allowed to stir overnight. The resulting brown suspension was filtered through Celite on a frit and evaporated to dryness *in vacuo*, to afford a brown residue. Recrystallisation from SiMe$_4$ at −35 °C afforded X-ray quality crystals of **1**.(SiMe$_4$)$_2$. Total yield: 744 mg (61% with respect to [K]$_2$Pn†). ^{1}H NMR (C$_6$D$_6$, 499.9 MHz, 303 K): δ_H 6.69 (2H, d, $^3J_{HH}$ = 2.5 Hz, Pn C*H*), 5.58 (2H, d, $^3J_{HH}$ = 2.5 Hz, Pn C*H*), 2.01 (30H, s, Cp* C*H$_3$*), 1.28 (6H, septet, $^3J_{HH}$ = 7.3 Hz, ^{i}Pr C*H*), 1.13 (36H, d, $^3J_{HH}$ = 7.3 Hz, ^{i}Pr C*H$_3$*). ^{13}C{^{1}H} NMR (C$_6$D$_6$, 125.7 MHz, 303 K): δ_C 138.3 (Pn bridgehead *C*), 114.7 (Cp*-*C*CH$_3$), 94.92 (Pn *C*H), 89.77 (Pn *C*-Si), 19.91 (^{i}Pr *C*H$_3$), 13.32 (^{i}Pr *C*H), 11.49 (Cp* C*C*H$_3$). ^{29}Si{^{1}H} NMR (C$_6$D$_6$, 79.4 MHz, 303 K): δ_{Si} −2.02. ^{171}Yb{^{1}H} NMR (C$_6$D$_6$, 69.9 MHz, 303 K): δ_{Yb} 59.9. EI-MS: *m/z* = 1004 (65%), [M − CCH$_3$]$^+$; 723 (15%), [M − YbCp*]$^+$. Anal. found (calcd. for C$_{46}$H$_{76}$Yb$_2$Si$_2$): C, 53.69 (53.57); H, 7.36 (7.43) %. Addition of 5 drops of THF to a C$_6$D$_6$ solution of **1** resulted in a brown solution, with a characteristic IR band at ν 1582 cm^{-1} and an ^{1}H NMR spectrum consistent with the known complex [Cp*Yb{THF}]$_2$(μ:η^5,η^5-Pn†).[17]

Synthesis of [Cp*Eu]$_2$(μ-Pn†) (2)

A solution of [K]$_2$Pn† (313 mg, 0.635 mmol) in toluene (30 mL) was added dropwise to a solution of Cp*Eu(BPh$_4$) (750 mg, 1.237 mmol) in a mixture of toluene-benzene (1:1 ratio, 60 mL) and allowed to stir overnight. The resulting orange suspension was filtered through Celite and the filtrate evaporated to dryness *in vacuo* to give an orange residue. Recrystallisation by slow evaporation of a toluene-pentane solution (1:3 ratio, 6 mL) at −35 °C afforded orange X-ray quality crystals of **2**.(C$_7$H$_8$). Duplicate microanalysis measurements on samples of powdered crystalline **2**.(C$_7$H$_8$)$_x$ from two independent facilities best fit to a value of *x* = 1.6. Total yield: 484 mg (68% with respect to [K]$_2$Pn†). EI-MS: *m/z* = 988 (45%), [M]$^+$; 853 (50%), [M − Cp*]$^+$. Anal. found (calcd. for C$_{46}$H$_{76}$Eu$_2$Si$_2$.(C$_7$H$_8$)$_{1.6}$): C, 60.59 (60.44); H, 8.02 (7.87) %. Mag. suscep. (Evans method, C$_6$D$_6$, 303 K): μ_{eff} = 7.64 μ_B per M; (SQUID, 300 K): μ_{eff} = 7.68 μ_B per M. Addition of 5 drops of THF to **2** resulted in an orange solution, with a characteristic IR band at ν 1145 cm^{-1} and a IR fingerprint matching that of an authentic sample of the known complex [Cp*Eu{THF}]$_2$(μ:η^5,η^5-Pn†).[17]

Synthesis of [Cp*Sm]$_2$(μ:η^5,η^5-Pn†) (3)

A solution [K]$_2$Pn† (471 mg, 0.957 mmol) in benzene (60 mL) was added dropwise to a solution of Cp*Sm(BPh$_4$) (1.159 g, 1.916 mmol) in benzene (30 mL) and allowed to stir for 8 h. The resulting brown-green suspension was filtered through Celite and the filtrate evaporated to dryness *in vacuo* to give a brown-green residue. Recrystallisation from pentane at −35 °C afforded X-ray quality crystals of **3**. In the solid state and solution, **3** slowly decomposes at room temperature to give a green compound, presumably (η^8-Pn†)SmCp*, and therefore requires storage at −35 °C or below. Total yield: 437 mg (46% with respect to [K]$_2$Pn†). ^{1}H NMR (C$_6$D$_6$, 499.9 MHz, 303 K, selected data): δ_H 20.09 (6H, br, ^{i}Pr C*H*), 15.53 (36H, br, ^{i}Pr C*H$_3$*), 10.15 (2H, br, Pn *H*), 7.50 (2H, br, Pn *H*), −2.71 (30H, s, Cp* C*H$_3$*). ^{13}C{^{1}H} NMR (C$_6$D$_6$, 125.7 MHz, 303 K): δ_C 24.50, 17.22, 6.45, −6.73, −24.04, −35.04, −45.84, −93.11. ^{29}Si{^{1}H} NMR (C$_6$D$_6$, 79.4 MHz, 303 K): δ_{Si} 117.7. EI-MS: *m/z* = 976–992 (principal peak 985, 25%), [M]$^+$; 696–705 (principal peak 701, 100%), [M − SmCp*]$^+$; 558–571 (principal peak 567, 35%), [M − SmCp*$_2$]$^+$. Anal. found (calcd. for C$_{46}$H$_{76}$Sm$_2$Si$_2$): C, 55.87 (56.03); H, 7.56 (7.77) %. Mag. suscep. (Evans method, toluene-*d*$_8$, 303 K): μ_{eff} = 3.04 μ_B per M; (SQUID, 300 K): μ_{eff} = 3.09 μ_B per M.

Synthesis of [Cp*Yb(OEt$_2$)$_3$][B(C$_6$F$_5$)$_4$] (4)

To a stirred suspension of **1** (79 mg, 0.077 mmol) in Et$_2$O (10 mL) at −40 °C was added [FeCp*$_2$][B(C$_6$F$_5$)$_4$] (77 mg, 0.077 mmol), and the resultant orange mixture was allowed to warm to room temperature. After 30 min the solvent was removed under reduced pressure to afford an orange-brown residue that was washed thoroughly with pentane (1 x 50, 2 x 5 mL) to remove FeCp*$_2$ until the washings were colourless. The residue was then extracted with Et$_2$O (4 mL), concentrated to *ca.* 3 mL and 5 drops of (Me$_3$Si)$_2$O were added. Cooling this solution to −35 °C produced yellow crystals that were isolated by decantation and dried *in vacuo*. Total yield: 63 mg (68% with respect to **1**). ^{1}H NMR (THF-*d*$_8$, 399.5 MHz, 303 K): δ_H 3.38 (12H, q, $^3J_{HH}$ = 7.0 Hz, OEt$_2$ C*H$_2$*), 1.97 (15H, s, Cp* C*H$_3$*), 1.11 (18H, t, $^3J_{HH}$ = 7.0 Hz, OEt$_2$ C*H$_3$*). ^{13}C{^{1}H} NMR (THF-*d*$_8$, 100.5 MHz, 303 K): δ_C 113.6 (Cp* ring *C*), 66.46 (OEt$_2$ *C*H$_2$), 15.82 (OEt$_2$ *C*H$_3$), 11.37 (Cp* *C*H$_3$). ^{19}F NMR (THF-*d*$_8$, 375.9 MHz, 303 K): δ_F −130.9 (br, *o-F*), −163.3 (t, $^3J_{FF}$ = 20.2 Hz, *p-F*), −166.8 (br t, $^3J_{FF}$ = 17.5 Hz, *m-F*). ^{11}B{^{1}H} NMR (THF-*d*$_8$, 128.2 MHz, 303 K): δ_B −14.74. ^{171}Yb{^{1}H} NMR (THF-*d*$_8$, 69.9 MHz, 303 K): δ_{Yb} 89.04. EI-MS: No volatility. Anal. found (calcd. for C$_{46}$H$_{45}$BF$_{20}$O$_3$Yb): C, 45.55 (45.67); H, 3.87 (3.75) %.

Synthesis of [(η^8-Pn†)Yb][K] (5)

THF (20 mL) was added to a solid mixture of YbI$_3$ (312 mg, 0.563 mmol) and [K]$_2$Pn† (276 mg, 0.563 mmol) and the resultant green suspension was stirred at room temperature for 4 h. Solid NaCp* (89 mg, 0.563 mmol) was added slowly, stirred at room temperature for 2 d and refluxed at 70 °C for 5 h. The mixture was stripped to dryness and the residues were extracted with pentane (3 x 4 mL) and filtered through Celite on a frit. The bright green filtrate was concentrated to *ca.* 2 mL and following storage at −35 °C produced green crystals, which were isolated by decantation and dried *in vacuo*. Total yield: 88 mg (15% with respect to [K]$_2$Pn†). ^{1}H NMR (THF-*d*$_8$, 399.5 MHz, 303 K): δ_H 4.90 (6H br, $\Delta\nu_{½}$ = 80 Hz, ^{i}Pr C*H*), 1.77 (36H br, $\Delta\nu_{½}$ = 58 Hz, ^{i}Pr C*H$_3$*), 1.10 (12H br, $\Delta\nu_{½}$ = 62 Hz, ^{i}Pr C*H*), −47.66

View Article Online
DOI: 10.1039/C6DT04475A

(4H br, $\Delta\nu_{½}$ = 550 Hz, Pn *H*). ^{13}C, ^{29}Si and ^{171}Yb NMR resonances were not observed due to the paramagnetic nature of **5**. EI-MS: *m/z* = 1042 (100%), $[M]^+$. Anal. found (calcd. for $C_{52}H_{92}KSi_4Yb$): C, 60.05 (59.95); H, 9.32 (8.90) %.

Crystallographic Details

Single crystal XRD data for **3** were collected by the UK National Crystallography Service (NCS),[79] at the University of Southampton on a Bruker-Nonius FR591 rotating anode diffractometer ($\lambda_{Mo\ K\alpha}$) equipped with VariMax VHF optics and a Saturn 724+ CCD area detector. The data were collected at 120 K using an Oxford Cryosystems Cobra low temperature device. Data collected by the NCS were processed using CrystalClear-SM Expert 3.1 b18,[80] and unit cell parameters were refined against all data. Single crystal XRD data for **1** and **2**, were collected at the University of Sussex on a Bruker-Nonius Kappa CCD area detector diffractometer with a sealed-tube source ($\lambda_{Mo\ K\alpha}$), in ω scanning mode with ψ and ω scans to fill the Ewald sphere. The data were collected at 173 K using an Oxford Cryosystems low temperature device. Data were processed using Collect,[81] Scalepack, and Denzo,[82] and unit cell parameters were refined against all data. An empirical absorption correction was carried out using the Multi-Scan program.[83] Solutions and refinements were performed using WinGX[84] and software packages within. All non-hydrogen atoms were refined with anisotropic displacement parameters. All hydrogen atoms were refined using a riding model.

Acknowledgements

We are grateful to the ERC (Project 247390), the EPSRC (EP/M023885/1), COST Action (CM1006) and the University of Sussex for financial support. We thank Dr A.-C. Schmidt (FAU Erlangen-Nürnberg) for assistance with SQUID measurements. Dr N. Tsoureas, Dr S. M. Roe (Sussex) and UK National Crystallography Service (Southampton) are acknowledged for their assistance with X-ray crystallography.

Notes and references

‡ Footnotes

1 T. Tsuji, N. Hosoya, S. Fukazawa, R. Sugiyama, T. Iwasa, H. Tsunoyama, H. Hamaki, N. Tokitoh and A. Nakajima, *J. Phys. Chem. C*, 2014, **118**, 5896–5907.
2 N. Hosoya, K. Yada, T. Masuda, E. Nakajo, S. Yabushita and A. Nakajima, *J. Phys. Chem. A*, 2014, **118**, 3051–3060.
3 N. Ishikawa, T. Iino and Y. Kaizu, *J. Am. Chem. Soc.*, 2002, **124**, 11440–11447.
4 J. J. Le Roy, M. Jeletic, S. I. Gorelsky, I. Korobkov, L. Ungur, L. F. Chibotaru and M. Murugesu, *J. Am. Chem. Soc.*, 2013, **135**, 3502–3510.
5 N. Magnani, C. Apostolidis, A. Morgenstern, E. Colineau, J.-C. Griveau, H. Bolvin, O. Walter and R. Caciuffo, *Angew. Chem. Int. Ed. Engl.*, 2011, **50**, 1696–1698.
6 S.-D. Jiang, B.-W. Wang, H.-L. Sun, Z.-M. Wang and S. Gao, *J. Am. Chem. Soc.*, 2011, **133**, 4730–4733.
7 G. A. Molander and J. A. C. Romero, *Chem. Rev.*, 2002, **102**, 2161–2186.
8 S. Kobayashi, M. Sugiura, H. Kitagawa and W. W.-L. Lam, *Chem. Rev.*, 2002, **102**, 2227–2302.
9 A. Avdeef, K. Raymond and K. Hodgson, *Inorg. Chem.*, 1972, **11**, 1083–1088.
10 A. M. Nonat, S. J. Quinn and T. Gunnlaugsson, *Inorg. Chem.*, 2009, **48**, 4646–4648.
11 S. Marks, J. G. Heck, M. H. Habicht, P. Oña-Burgos, C. Feldmann and P. W. Roesky, *J. Am. Chem. Soc.*, 2012, **134**, 16983–16986.
12 O. T. Summerscales and F. G. N. Cloke, *Coord. Chem. Rev.*, 2006, **250**, 1122–1140.
13 J. M. Manriquez, M. D. Ward, W. M. Reiff, J. C. Calabrese, N. L. Jones, P. J. Carroll, E. E. Bunel and J. S. Miller, *J. Am. Chem. Soc.*, 1995, **117**, 6182–6193.
14 B. Oelckers, I. Chávez, J. M. Manríquez and E. Roman, *Organometallics*, 1993, **12**, 3396–3397.
15 Y. Portilla, I. Chavez, V. Arancibia, B. Loeb, J. M. Manríquez, A. Roig and E. Molins, *Inorg. Chem.*, 2002, **41**, 1831–1836.
16 E. E. Bunel, L. Valle, N. L. Jones, P. J. Carroll, C. Barra, M. Gonzalez, N. Munoz, G. Visconti, A. Aizman and J. M. Manriquez, *J. Am. Chem. Soc.*, 1988, **110**, 6596–6598.
17 O. T. Summerscales, S. C. Jones, F. G. N. Cloke and P. B. Hitchcock, *Organometallics*, 2009, **28**, 5896–5908.
18 O. T. Summerscales, D. R. Johnston, F. G. N. Cloke and P. B. Hitchcock, *Organometallics*, 2008, **27**, 5612–5618.
19 H. Schumann, M. Glanz, H. Hemling and F. H. Görlitz, *J. Organomet. Chem.*, 1993, **462**, 155–161.
20 W. J. Evans, T. A. Ulibarri, L. R. Chamberlain, J. W. Ziller and D. Alvarez, *Organometallics*, 1990, **9**, 2124–2130.
21 W. J. Evans, K. J. Forrestal and J. W. Ziller, *J. Am. Chem. Soc.*, 1998, **120**, 9273–9282.
22 W. J. Evans, T. M. Champagne and J. W. Ziller, *Organometallics*, 2007, **26**, 1204–1211.
23 W. J. Evans, J. R. Walensky, F. Furche, A. G. DiPasquale and A. L. Rheingold, *Organometallics*, 2009, **28**, 6073–6078.
24 W. J. Evans, J. Walensky and T. Champagne, *J. Organomet. Chem.*, 2009, **694**, 1238.
25 M. Schultz, C. J. Burns, D. J. Schwartz and R. A. Andersen, *Organometallics*, 2000, **19**, 781–789.
26 D. J. Berg, C. J. Burns, R. A. Andersen and A. Zalkin, *Organometallics*, 1989, **8**, 1865–1870.
27 D. J. Schwartz and R. A. Andersen, *Organometallics*, 1995, **14**, 4308–4318.
28 J. Mason, *Chem. Rev.*, 1987, **87**, 1299–1312.
29 P. B. Hitchcock, M. F. Lappert and S. Tian, *Organometallics*, 2000, **19**, 3420–3428.
30 J. M. Keates, G. A. Lawless and M. P. Waugh, *Chem. Commun.*, 1996, 1627–1628.
31 A. Edelmann, S. Blaurock, V. Lorenz, L. Hilfert and F. T. Edelmann, *Angew. Chem. Int. Ed.*, 2007, **46**, 6732–6734.
32 W. J. Evans, M. A. Johnston, M. A. Greci and J. W. Ziller, *Organometallics*, 1999, **18**, 1460–1464.
33 W. J. Evans, M. A. Johnston, R. D. Clark and J. W. Ziller, *J. Chem. Soc., Dalton Trans.*, 2000, 1609–1612.
34 W. J. Evans, M. Johnston, R. Clark, R. Anwander and J. Ziller, *Polyhedron*, 2001, **20**, 2483–2490.
35 N. G. Connelly and W. E. Geiger, *Chem. Rev.*, 1996, **96**,

View Article Online
DOI: 10.1039/C6DT04475A

877–910.
36 W. J. Evans, L. A. Hughes and T. P. Hanusa, *Organometallics*, 1986, **5**, 1285–1291.
37 C. J. Burns and R. A. Andersen, *J. Organomet. Chem.*, 1987, **325**, 31–37.
38 T. P. Hanusa, *Chem. Rev.*, 1993, **93**, 1023–1036.
39 R. D. Shannon, *Acta. Crystallogr. Sect. A.*, 1976, **32**, 751–767.
40 T. D. Tilley, R. A. Andersen, B. Spencer, H. Ruben, A. Zalkin and D. H. Templeton, *Inorg. Chem.*, 1980, **19**, 2999–3003.
41 W. J. Evans, J. W. Grate, H. W. Choi, I. Bloom, W. E. Hunter and J. L. Atwood, *J. Am. Chem. Soc.*, 1985, **107**, 941–946.
42 W. J. Evans, R. D. Clark, M. A. Ansari and J. W. Ziller, *J. Am. Chem. Soc.*, 1998, **120**, 9555–9563.
43 O. T. Summerscales, S. C. Jones, F. G. N. Cloke and P. B. Hitchcock, 2009, **28**, 5896–5908.
44 W. J. Evans, L. A. Hughes and T. P. Hanusa, *J. Am. Chem. Soc.*, 1984, **106**, 4270–4272.
45 T. D. Tilley, R. A. Andersen and A. Zalkin, *J. Am. Chem. Soc.*, 1982, **104**, 3725–3727.
46 T. D. Tilley, R. A. Andersen and A. Zalkin, *Inorg. Chem.*, 1984, **23**, 2271–2276.
47 J. M. Boncella and R. A. Andersen, *Organometallics*, 1985, **4**, 205–206.
48 W. J. Evans, D. K. Drummond, H. Zhang and J. L. Atwood, *Inorg. Chem.*, 1988, **27**, 2904–2904.
49 P. B. Hitchcock, S. A. Holmes and M. F. Lappert, *J. Chem. Soc., Chem. Commun.*, 1994, 2691–2692.
50 Z. Feng, X. Zhu, S. Wang, S. Wang, S. Zhou, Y. Wei, G. Zhang, B. Deng and X. Mu, *Inorg. Chem.*, 2013, **52**, 9549–9556.
51 G. B. Deacon, P. C. Junk and G. J. Moxey, *Chem.–Eur. J.*, 2009, **15**, 5503–5519.
52 F. G. N. Cloke and P. B. Hitchcock, *J. Am. Chem. Soc.*, 2002, **124**, 9352–9353.
53 J. C. Green, M. L. H. Green and G. Parkin, *Chem. Commun.*, 2012, **48**, 11481–11503.
54 J. Evans, *J. Chem. Soc.*, 1959, 2003–2005.
55 E. M. Schubert, *J. Chem. Educ.*, 1992, **69**, 62.
56 A. F. Orchard, *Magnetochemistry*, Oxford University Press, 2003.
57 J. J. Le Roy, L. Ungur, I. Korobkov, L. F. Chibotaru and M. Murugesu, *J. Am. Chem. Soc.*, 2014, **136**, 8003–8010.
58 T. Fukuda, W. Kuroda and N. Ishikawa, *Chem. Commun.*, 2011, **47**, 11686–11688.
59 J. H. Van Vleck, *The Theory of Electric and Magnetic Susceptibilities*, Clarendon Press, 1932.
60 N. M. Edelstein, T. J. Marks and R. D. Fischer, *Organometallics of the f Elements*, D. Reidel, Dordrecht, 1979.
61 N. Edelstein, T. J. Marks, I. L. Fragala and D. Reidel, *Fundamental and Technological Aspects of Organo-f-Element Chemistry*, D. Reidel, Dordrecht, 1985.
62 W. E. Geiger, *Organometallics*, 2007, **26**, 5739.
63 L. R. Morss, *Chem. Rev.*, 1976, **76**, 827–841.
64 C. J. Kuehl, R. E. Da Re, B. L. Scott, D. E. Morris and K. D. John, *Chem. Commun.*, 2003, 2336–2337.
65 J. M. Veauthier, E. J. Schelter, C. N. Carlson, B. L. Scott, R. E. D. Re, J. D. Thompson, J. L. Kiplinger, D. E. Morris and K. D. John, *Inorg. Chem.*, 2008, **47**, 5841–5849.
66 P. L. Watson and T. H. Tulip, *Organometallics*, 1990, **9**, 1999–2009.
67 R. G. Compton and C. E. Banks, *Understanding Voltammetry*, Imperial College Press, 2nd edn. 2011.
68 W. E. Geiger and F. Barrière, *Acc. Chem. Res.*, 2010, **43**, 1030–1039.
69 G. B. Deacon and C. M. Forsyth, *Chem. Commun.*, 2002, 2522–2523.
70 G. B. Deacon, C. M. Forsyth and P. C. Junk, *Eur. J. Inorg. Chem.*, 2005, **2005**, 817–821.
71 G. Balazs, F. G. N. Cloke, J. C. Green, R. M. Harker, A. Harrison, P. B. Hitchcock, C. N. Jardine and R. Walton, *Organometallics*, 2007, **26**, 3111–3119.
72 A. Ashley, G. Balazs, A. Cowley, J. Green, C. H. Booth and D. O'Hare, *Chem. Commun.*, 2007, 1515–1517.
73 F. G. N. Cloke, M. C. Kuchta, R. M. Harker, P. B. Hitchcock and J. S. Parry, *Organometallics*, 2000, **19**, 5795–5798.
74 G. Rabe, H. W. Roesky, D. Stalke, F. Pauer and G. M. Sheldrick, *J. Organomet. Chem.*, 1991, **403**, 11–19.
75 N. M. Kuuloja, T. M. Kylmälä, J. E. Tois, R. E. Sjöholm and R. G. Franzén, *Synth. Commun.*, 2011, **41**, 1052–1063.
76 T. D. Tilley, J. M. Boncella, D. J. Berg, C. J. Burns and R. A. Andersen, *Inorg. Synth.*, 1990, **27**, 146.
77 E. W. Washburn, *International Critical Tables*, McGraw-Hill, New York, 1929, vol. 3.
78 D. Ostfeld and I. A. Cohen, *J. Chem. Educ.*, 1972, **49**, 829.
79 S. J. Coles and P. A. Gale, *Chem. Sci.*, 2012, **3**, 683–689.
80 Rigaku, *CrystalClear*, 2011.
81 Bruker-AXS BV, *Collect*, 1997.
82 Z. Otwinowski and W. Minor, *Methods Enzymol.*, 1997, **276**, 307–326.
83 R. H. Blessing, *Acta Crystallogr., A, Found. Crystallogr.*, 1995, **51**, 33–38.
84 L. J. Farrugia, *J. Appl. Crystallogr.*, 1999, **32**, 837–838.

View Article Online
DOI: 10.1039/C6DT04475A

Homobimetallic complexes of Yb, Eu and Sm bridged by a silylated pentalene ligand have been prepared and intermetallic communication studied by magnetic measurements and cyclic voltammetry.